Clinical Neurophysiology 126 (2015) 505–513

Contents lists available at ScienceDirect

Clinical Neurophysiology

journal homepage: www.elsevier.com/locate/clinph

Quantitative EEG markers relate to Alzheimer's disease severity in the Prospective Dementia Registry Austria (PRODEM)

Heinrich Garn [a,*], Markus Waser [a], Manfred Deistler [b], Thomas Benke [c], Peter Dal-Bianco [d], Gerhard Ransmayr [e], Helena Schmidt [f], Guenter Sanin [c], Peter Santer [d], Georg Caravias [e], Stephan Seiler [f], Dieter Grossegger [g], Wolfgang Fruehwirt [g], Reinhold Schmidt [f]

[a] AIT Austrian Institute of Technology GmbH, Vienna, Austria
[b] Vienna University of Technology, Vienna, Austria
[c] Department of Neurology, Innsbruck Medical University, Innsbruck, Austria
[d] Department of Neurology, Vienna Medical University, Vienna, Austria
[e] Department of Neurology, Linz General Hospital, Linz, Austria
[f] Department of Neurology, Graz Medical University, Graz, Austria
[g] Dr. Grossegger & Drbal GmbH, Vienna, Austria

ARTICLE INFO

Article history:
Accepted 7 July 2014
Available online 12 July 2014

Keywords:
PRODEM
Alzheimer's disease
Quantitative electroencephalogram

HIGHLIGHTS

- Largest clinical study of quantitative EEG markers for slowing, synchrony and complexity versus AD severity including 118 patients.
- Advanced metrics for quantitative EEG in resting state and during a face–name encoding task.
- MMSE scores explaining up to 51% of the variations in QEEG markers.

ABSTRACT

Objective: To investigate which single quantitative electro-encephalographic (QEEG) marker or which combination of markers correlates best with Alzheimer's disease (AD) severity as measured by the Mini–Mental State Examination (MMSE).
Methods: We compared quantitative EEG markers for slowing (relative band powers), synchrony (coherence, canonical correlation, Granger causality) and complexity (auto-mutual information, Shannon/Tsallis entropy) in 118 AD patients from the multi-centric study PRODEM Austria. Signal spectra were determined using an indirect spectral estimator. Analyses were adjusted for age, sex, duration of dementia, and level of education.
Results: For the whole group (39 possible, 79 probable AD cases) MMSE scores explained 33% of the variations in relative theta power during face encoding, and 31% of auto-mutual information in resting state with eyes closed. MMSE scores explained also 25% of the overall QEEG factor. This factor was thus subordinate to individual markers. In probable AD, QEEG coefficients of determination were always higher than in the whole group, where MMSE scores explained 51% of the variations in relative theta power.
Conclusions: Selected QEEG markers show strong associations with AD severity. Both cognitive and resting state should be used for QEEG assessments.
Significance: Our data indicate theta power measured during face–name encoding to be most closely related to AD severity.

1. Introduction

Numerous studies have investigated quantitative electroencephalogram (QEEG) measures as a tool for differentiating between

* Corresponding author. Tel.: +43 50550 4103.
E-mail address: Heinrich.garn@ait.ac.at (H. Garn).

http://dx.doi.org/10.1016/j.clinph.2014.07.005
1388-2457/

normal controls (NC) and patients with Alzheimer's disease (AD) (Drago et al., 2011; Sakkalis, 2011; Platt and Riedel, 2011; Leiser et al., 2011; Santos et al., 2010; Dauwels et al., 2010; Giannakopoulos et al., 2009; Rossini et al., 2007; Uhlhaas and Singer, 2006; Menendez, 2005; Jeong, 2004). Moreover, several studies have investigated the implications of QEEG in predicting progression from mild cognitive impairment to AD, but only two longitudinal studies have looked at AD progression (Soininen et al., 1991; Coben et al., 1985).

The majority of studies consistently found a "slowing" in the frequency spectrum, i.e. a shift in signal power to lower frequencies in AD patients as compared to controls. Some studies also reported altered synchrony between sites across the cortex and reduced signal complexity. A comprehensive discussion of hypotheses about the pathophysiological origin of abnormal EEG has been reported in the review by Jeong (2004) (in extracts):

"Slowing is assumed to be caused by cholinergic deficit. AD is thought to be a syndrome of neocortical disconnection, in which profound cognitive losses arise from the disrupted structural and functional integrity of long cortico-cortical tracts. Senile plaques and neurofibrillary tangles of AD prominently involve the origins and terminations of long cortico-cortical association fibers. The atrophy of basal forebrain cholinergic neurons innervating the neocortex and hippocampus might play a critical role in the EEG slowing of AD.

EEG signals are generated by nonlinear coupling interactions between neuronal populations. Neuronal death, deficiency of neurotransmitters like acetylcholine, and/or loss of connectivity of local neuronal networks might cause decreased dynamic complexity of the EEG in AD patients. A loss of dynamical brain responsivity to stimuli might be another reason. Therefore, the reduced EEG complexity in AD suggests the deficient information processing of the cortex due to the inactivation of previously active networks.

Decreased synchrony reflects reduced functional connections between cortical areas beneath the electrodes or reduced common modulation of two areas. This might result from a loss of long cortico-cortical association fibers. In addition, a decrease in synaptic couplings can reduce long-distance functional connections even when the anatomical connections are intact. A distinct feature of AD is a loss of acetylcholine, an excitatory neurotransmitter of the cerebral cortex. Thus, it is possible that the decrease in EEG synchrony of AD results from both anatomical disconnections among different cortical regions and reduced cholinergic coupling interactions between cortical neurons."

The purpose of the current study was to investigate which individual QEEG marker or combination of markers correlates best with AD severity as measured by the Mini–Mental State Examination (MMSE) (Folstein et al., 1975; Rosen et al., 1984).

Unlike most previous investigations that were done in resting state, our study also included QEEG assessments during execution of a face–name encoding task. Previous studies that investigated the EEGs of AD patients during cognitive demands for the brain used a Sternberg-type memory scanning task with three levels: working memory load (Hogan et al., 2003), reverse counting (Hidasi et al., 2007), and a visual working memory task (Pijnenburg et al., 2004). Those studies did not investigate markers versus disease severity. Moreover, with less than 20 patients each, their sample sizes were small.

We here present QEEG data for 118 AD cases involving thorough signal preprocessing and use of a semi-automated procedure for epoch selection, artifact detection and removal. Moreover, we applied an indirect spectral estimator to determine multivariate signal spectra of short epochs that provided variances for large samples lower than the commonly used periodogram and that allowed us to analyze with high accuracy the relationships between QEEG markers and MMSE scores.

2. Methods

2.1. Ethics statement

The study was approved by the ethics committees of the Medical Universities of Graz, Innsbruck and Vienna, and by the Ethics Committee of the State of Upper Austria. Written informed consent was obtained from all patients and their caregivers.

2.2. Subjects of the Prospective Dementia Database Austria (PRODEM)

Subjects were patients at the neurological departments of the Medical Universities of Graz, Innsbruck and Vienna and Linz General Hospital, Austria, all of whom participated in the Prospective Dementia Database Austria (PRODEM). PRODEM is an ongoing longitudinal multi-center cohort study of patients with Alzheimer's disease (Seiler et al., 2012). Inclusion criteria were (1) diagnosis of Alzheimer-type dementia according to NINCDS-ADRDA criteria (McKhann et al., 1984), (2) minimum age 40 years, (3) non-institutionalization and no need for 24-hour care, (4) availability of a caregiver who agrees to provide information on the patient's condition. Exclusion criteria were the inability to sign an informed consent form or the existence of co-morbidities likely to preclude termination of the study. The current cohort consists of 118 patients with possible (29) or probable (79) AD. Median age was 76 years and median duration of illness 12 months. There were 74 (69%) women enrolled. MMSE scores ranged from 15 to 26. Median AD duration was one year. Seventy-five (63.6%) patients had arterial hypertension, 14 (11.9%) diabetes mellitus, 16 (13.6%) coronary heart disease, nine (7.6%) atrial fibrillation, 50 (42.4%) had hypercholesterolemia, 28 (23.7%) were former or current smokers and 36 (30.5%) reported former or current alcohol consumption on a regular basis. Demographic data and risk factors are summarized in Table 1. About 30% of the patients were treated with acetylcholinesterase inhibitors and less than 1% with memantine at the time of EEG recordings.

The following neuropsychological tests were performed: Mini–Mental State Examination (MMSE), Clinical Dementia Rating (CDR), Neuropsychiatric Inventory (NPI), Neuropsychologic Test Battery CERAD-NP and CERAD-Plus, Geriatric Depression Scale (GDS), Disability Assessment for Dementia Scale (DAD). We calculated a CERAD total score in a fashion similar to Chandler (Chandler et al., 2005), but used the sum of z-values of the CERAD items "verbal fluency", "Boston Naming Test", "word list learning", "constructional praxis", "word list recall" and "discriminability". Results are summarized in Table 1.

Furthermore, MRI scans were performed, but MRI data have yet not been analyzed. The association between quantitative EEG data and global as well as regional atrophy measures will be disclosed once automated MRI measurements are available.

2.3. Paradigms for EEG assessment

Our paradigm included resting state with eyes closed and a face–name encoding task. For this "cognitive EEG" we used selected activities, in which AD patients show disease-specific deficits including episodic memory and processing of complex stimuli.

It was not the purpose to test these deficits but just to engage the patient's attention in encoding of new information. The number of faces was limited to three because of limited cognitive capabilities of AD patients.

The following recording periods were designed and implemented in a computer-controlled procedure:

A: Resting state with eyes closed (RSEC, 180 s)

B: Resting state with eyes open (180 s)

Table 1
Demographic parameters, neuropsychological parameters and risk factors of the study population.

	Whole AD group			Probable AD group		
	Range	Median	Median abs. deviation	Range	Median	Median abs. deviation
Demographic parameters						
Sex (m/f)	44 m, 74 f			29 m, 50 f		
Age (years)	52–90	76	5	52–88	75	6
Level of education (scale 1–6)	1–6	1.5	0.5	1–6	2	1
Duration of illness (months)	2–120	12	12	2–120	23	13
Neuropsychological parameters						
MMSE score (scale 30–0)	26–15	23	2	26–15	22	2
CDR (0–0.5–1–2–3)	0–2	0.5	0	0–2	0.5	0
NPI total score	0–53	5	5	0–49	4	4
DAD (0–100%)	30–100	82.5	15	30–100	86.25	13.75
GDS	0–11	2	1	0–11	2	1
CERAD total *z*-scores	-23.8 to +1.4	−9.2	3.2	-21.8 to +1.4	−10.5	3.45

Risk factors	Frequency of occurrence, whole group	Frequency of occurrence, probable AD
	N = 118	*N* = 79
Arterial hypertension	63.6% yes, 32.2% no, 4.2% unknown	57.0% yes, 39.2% no, 3.8% unknown
Diabetes mellitus	11.9% yes, 84.7% no, 3.4% unknown	12.7% yes, 84.8% no, 2.5% unknown
Coronary heart disease	13.6% yes, 82.2% no, 4.2% unknown	10.1% yes, 86.1% no, 3.8% unknown
Atrial fibrillation	7.6% yes, 84.7% no, 7.6% unknown	5.1% yes, 98.7% no, 6.3% unknown
Hypercholesterolemia	42.4% yes, 50.8% no, 6.8% unknown	36.7% yes, 57.0% no, 6.3% unknown
Nicotine	72.9% never, 20.3% earlier, 3.4% now, 3.4% unknown	74.7% never, 17.7% earlier, 2.5% now, 5.1% unknown
Alcohol	66.1% never, 8.5% earlier, 22.2% now, 3.4% unknown	64.6% never, 7.6% earlier, 22.8% now, 5.1% unknown

C: Encoding of three faces and corresponding names with eyes open (FNET). This comprised three sub-periods:

1. Faces and corresponding names presented on a computer screen (50 s).
2. Each face presented without the corresponding name while the patient is asked to recall the respective name (30 s on average).
3. Faces and corresponding names shown simultaneously again (50 s).

The EEGs from period B were not used for the assessments.

2.4. EEG data acquisition

Patients sat in an upright position in a comfortable chair with neck rest. A 21-inch computer screen was placed in front of their face at a comfortable distance for the patient. The room was well illuminated, quiet and had a pleasant temperature. The door was closed and no disturbances were permitted during the recordings.

EEG data were collected from the 19 monopolar electrode sites of the International 10/20 System using gold cup electrodes and adhesive covered with gaze pads. Data acquisition was performed on an AlphaEEG amplifier (alpha trace medical systems, Vienna, Austria) with NeuroSpeed software (alpha trace medical systems).

Electrodes for the horizontal electro-oculogram (HEOG) were placed at the outer corner of the right and left eye. Electrodes for the vertical electro-oculogram (VEOG) were aligned vertically above and below the left eye. The ground electrode was placed at FCz. Connected mastoid electrodes were preferred as reference, because they provide a reference potential that contains less brain signals than common average.

At the beginning of each session, an automated impedance test was performed and electrode contacts were arranged to achieve impedances below 10 kiloohms. The EEG amplifiers had a band pass of 0.3 to 70 Hz (3 dB points) with a 50 Hz notch filter. Data were sampled at a rate of 256 s^{-1} with 16 bits resolution. The electrocardiography (ECG) signal was recorded via clamp electrodes around both wrists.

The number of channels (19) and the digitization rate (256 s^{-1}) are standard in today's clinical practice. These numbers are sufficient for computing the qEEG markers used in this study.

2.5. EEG preprocessing

EEG data require careful, extensive preprocessing before reliable QEEG assessments can be made. Our preprocessing procedure included the following steps:

In the first step, usable sections of EEG were visually selected by an experienced expert as follows: Sections with artifacts caused by patient movement or talking or by poor electrode contacts that appeared as excessive voltage were excluded from further assessment.

RSEC: On average, 158 s out of 180 s were used for processing (87.8%).

FNET: On average, 86 s out of 130 s were used for processing (66.2%).

The computer program used to monitor the test procedure sets markers between each of the periods of the paradigm. Selected sections had to be between these markers and had to be longer than four seconds with no maximum duration, because segmentation was performed automatically later in the procedure.

Artifacts from eye movement and blinking and from heartbeat were automatically corrected in most cases:

Interference from eye movement and blinking was eliminated from the EEG channels by linear regression (Draper and Smith, 1966) using the horizontal and vertical electro-oculogram (H-EOG, V-EOG) signals. In contrast to independent component analysis, regression represents a precise method to remove particular undesired signal components.

The patient's heartbeat causes electric fields that extend up to the head. These fields are picked up by the EEG leads connected to the high-impedance input of the EEG amplifier. This causes tiny voltage peaks to appear in the EEG signals and thus distort the qEEG markers (Waser and Garn, 2013). The peaks can be identified by their synchrony to the QRS complex in the ECG channel. To detect and correct interference caused by the electromagnetic fields of the patient's heartbeat we used a modified Pan-Tompkins algorithm and linear regression. This method was previously described (Waser and Garn, 2013). It is able to eliminate artifacts from the heartbeat in typically more than 85% of all patients and fails only if the heartbeat-induced peaks in EEG deviate in synchrony or shape from the QRS complexes of the ECG signal. Patients in whom this problem occurred were excluded from assessment.

In some of the EEG data we observed slow fluctuations in EEG signals with frequencies between about 0.5 and 1.5 Hz. These were mostly caused by sweating. We thus used 2 Hz high-pass filtering to eliminate such fluctuations.

When no further interference was detected after artifact correction, a sliding window (length 4 s, overlap 2 s) was automatically moved over the artifact-free, interference-corrected sections of the EEG to determine series of 4-second epochs with an overlap of 2 s. These epochs were used to calculate the EEG markers for each period.

2.6. EEG markers used in this study

Since our patients sat in upright position during EEG assessment, muscle activity in temporal electrodes could not be avoided. This activity caused intensified beta oscillations in temporal electrodes at frequencies above 15 Hz. Therefore, we limited the assessments to 15 Hz at these electrodes (T7, T8, F7, F8, P7, P8).

Electrode clusters for regions of the cortex were defined as follows (Dauwels et al., 2010): anterior: Fp1, Fp2, F3, F4; central: Fz, Cz, Pz, C3, C4; temporal: F7, T7, P7 (left side) and F8, T8, P8 (right side); posterior: P3, P4, O1, O2; posterior-temporal: P7, P3, O1, P8, P4, O2; anterior-temporal: Fp1, F3, F7, Fp2, F4, F8.

Markers were calculated on 19 individual electrodes. In addition, markers were calculated on first and second principal components (Hotelling, 1933) of the above electrode clusters.

All computations were performed using Matlab R 2011a.

2.6.1. Slowing measures

We calculated *relative band powers* in the delta (2–4 Hz), theta (4–8 Hz), alpha (8–13 Hz), and beta1 (13–20 Hz; for T7, T8, F7, F8, P7, P8 only 13–15 Hz) bands.

We used an indirect spectral estimator (Brillinger, 1981) to determine the spectral density of each of the selected epochs. For this purpose, Fourier transformation was not applied to the original time signal, but to its covariance function as demonstrated in (Waser et al., 2013). By using a so-called lag-window, covariances with greater time lags were weighted less than were those with smaller time lags. We used the well-established Parzen window (Brillinger, 1981), because it guarantees non-negativity of the spectral estimate.

Once the spectral density was determined, the power in a particular frequency band was calculated from the sum of squared amplitudes in that frequency band. Values for each frequency band were expressed as percentage of the power in the total 2–20 Hz range.

The reason why an indirect spectral estimator was used is that the periodogram has considerable disadvantages for this application: (i) It offers only limited frequency resolution (0.25 Hz with 4 s epochs); (ii) the periodogram is not consistent because its variance does not converge to zero; (iii) the values of the periodogram at consecutive frequencies are independent of each other. For this reason periodograms always show a significant "ripple" in the trace. This effect does not reflect the true spectral density, but can be explained by the mentioned basic mathematical phenomena. Finally, leakage of window functions causes additional errors (albeit minor than for the mentioned variances).

2.6.2. Measures for altered synchrony

All synchrony measures were calculated for the following pairs of electrodes: Fp1-O1, Fp2-O2, Fp1-P3, Fp2-P4, F3-O1, F4-O2, F3-P3, F4-P4, C3-O1, C4-O2, F7-F8, F3-F4, T7-T8, C3-C4, P7-P8, P3-P4, O1-O2, Fp1-F7, Fp2-F8, Fp1-F3, Fp2-F4, F7-C3, F8-C4, F7-T7, F8-T8, F3-C3, F3-C4, P7-O1, P8-O2, P3, O1, P4-O2, C3-P7, C4-P8, P3-C3, P4-C4, P3-P7, P4-P8;

In addition, all synchrony measures were calculated between the following pairs of electrode clusters (Table 1): anterior-central, anterior-posterior, anterior-temporal/left, anterior-temporal/right, central-posterior, central-temporal/left, central-temporal/right, posterior-temporal/left, posterior-temporal/right, temporal/left-temporal/right, anterior/temporal-posterior/temporal, left-right.

Coherences were calculated according to frequency and averaged in the frequency ranges delta (2–4 Hz), theta (4–8 Hz), alpha (8–13 Hz), and beta1 (13–20 Hz; for T7, T8, F7, F8, P7, P8 only 13–15 Hz) between selected pairs of individual electrodes.

Coherence (Rosenberg et al., 1989) between the ith and jth channel at frequency f was calculated from the spectral densities of these channels and their cross-spectral density.

Conditional Granger causalities (Flamm et al., 2012) were calculated for selected pairs of individual electrodes on band-limited (2–15 Hz) signals.

A channel i is considered to be Granger-causal for channel j, if the knowledge about the past of channel i improves the prediction of future values of channel j (Granger, 1969).

Static canonical correlation (Hotelling, 1936) was calculated from the auto-covariance function of two electrode clusters on band-limited (2–15 Hz) signals.

Canonical correlation between electrode clusters i and j is defined as the maximum correlation between linear combinations of clusters i and j and can thus be used as measure of synchrony between these clusters.

2.6.3. Measures for reduced complexity

Auto-mutual information (Cover and Thomas, 1991) was calculated in the frequency range 2–15 Hz. Auto-mutual information measures the mutual dependence of a time signal and its time-shifted version.

Entropy measures the predictability of a random variable and can thus be used to quantify the complexity of a signal. The *Shannon entropy* (Shannon, 1948) and *Tsallis entropy* (Tsallis, 1988) were calculated in the frequency range 2–15 Hz.

Averaging of the epochs

For each electrode, results for all selected epochs were averaged in each period. The number of usable epochs depended on the quality of electrode contacts and possible technical artifacts and varied from patient to patient. For the three-minute period in resting state with eyes closed the mean number of epochs was 78 ± 14 (1 SD). For the face–name encoding task it was 43 ± 16.

2.6.4. Factor analyses

Factors were calculated with the maximum likelihood approach (Lawley, 1940) for each of the three categories of EEG markers, namely slowing (relative theta band power on left-side electrode cluster, 2nd component, FNET; alpha relative band power on electrode P7, RSEC; beta1 relative band power on electrode C3, FNET); synchrony (delta between central and left temporal electrode cluster, 2nd component, FNET; conditional Granger causality (past) between central and posterior electrode clusters, 1st component, RSEC; static canonical correlation between central and left temporal electrode clusters, FNET), and complexity (auto-mutual information on left-side electrode cluster, 2nd component, RSEC; Shannon entropy on electrode T7, RSEC; Tsallis entropy on electrode T7, RSEC). In addition, an overall QEEG factor was determined for both the whole AD group and the subgroup of probable AD patients.

2.6.5. Statistical analyses of the relationships between MMSE scores and EEG markers

Analyses were adjusted for the co-variables age, sex, duration of dementia, and level of education. Age and duration of dementia were introduced via linear and quadratic terms. With the

exception of treatment with AChEI (1/0) and APOE epsilon 4 carriers (one or two allele versus no allele), all individual linear terms were statistically significant. Among the quadratic terms, only age was significant. Cross terms were not significant.

Medians and least medians of squares were used because of skewed data distributions.

We used scatter plots to visualize the distribution of EEG parameters versus MMSE. Quadratic univariate regressions were fitted to these scatter plots. EEG markers were the dependent variables. Fisher's F test was used to determine statistical significance in the regressions. Coefficients of determination (R^2) were calculated to evaluate the extent to which variations in EEG markers can be explained by MMSE scores markers.

3. Results

Band powers, coherences, canonical correlations, Granger causalities, auto-mutual information, Shannon entropy and Tsallis entropy were calculated for resting state with eyes closed (RSEC) and the face–name encoding task (FNET). Table 2 summarizes the results for the whole AD group and for the subgroup probable AD patients. The table demonstrates coefficients of determination by cortical region and by cognitive task. With the exception of entropies, higher coefficients of determination were found for electrode clusters than for individual electrodes. Fig. 1 shows distributions of p-values and coefficients of determination on the cortex for selected markers.

3.1. Probable and possible AD combined

The highest coefficient of determination between QEEG marker and MMSE score was found for the theta (4–8 Hz) relative band power. As shown in Fig. 2, relative theta power increased with decreasing MMSE score. In the second components of the left-side electrode cluster, 33% of the variation in relative theta power (FNET) was explained by MMSE scores.

Table 2
Electrodes and electrode clusters with statistically significant results ($p < 0.0036 = 0.05/14$) after Bonferroni correction and coefficients of determination for electrode sites and 1st/2nd components of electrode clusters.

Slowing		2nd component – whole AD group		2nd component – probable AD group	
Rel. band power		Clusters $p < 0.0036$	Highest R^2	Clusters $p < 0.0036$	Highest R^2
Delta	RSEC	All except An	0.21: L	An-Te, Po, Po-Te, Te/L, L	0.27: Po-Te,L
	FNET	None	–	None	–
Theta	RSEC	All	0.28: Te/L	All	0.42 Te/L
	FNET	All except An,An-Te	0.33: L	All except An&An-Te	0.51 L
Alpha	RSEC	All except An,An-Te	0.21 Te/L	Po, Po-Te, Te/L	0.24 Po-Te
	FNET	None	–	None	–
Beta1	RSEC	An-Te,Po,Po-Te,Te/L	–	All	0.27 Te/L
	FNET	All except An,An-Te,R	0.25: Po-Te	All except An&An-Te	0.35 L

Synchrony		2nd component – whole AD group		2nd component – probable AD group	
Coherence		Clusters $p < 0.0036$	Highest R^2	Clusters $p < 0.0036$	Highest R^2
2–15 Hz	RSEC	None	–	None	–
	FNET	Ce-TL	–	Ce-TL	0.40: Ce-TL
Delta	RSEC	None	–	Ce-TL,Ce-TR	0.23 Ce-TL
	FNET	Ce-TL	–	Ce-TL	0.41 Ce-TL
Theta	RSEC	None	–	None	–
	FNET	Ce-TL	–	Ce-TL,Po-TL	0.36: Ce-TL
Alpha	RSEC	None	–	None	–
	FNET	None	–	Ce-TL	0.37 Ce-TL
Beta1	RSEC	None	–	None	–
	FNET	Ce-TL	–	Ce-TL	0.22: Ce-TL
		1st component – whole AD group		1st component – probable AD group	
Condit. Granger causality (past)		Clusters $p < 0.0036$	Highest R^2	Clusters $p < 0.0036$	Highest R^2
2–15 Hz	RSEC	An-Po,Ce-Po	–	An-Ce,An-Po,An-TL,TL-An,Ce-Po,Pos-Ce,Ce-TL,TL-Ce,TL-Po,TR-Po,TL-TR,TR-TL	0.41: Ce-Po
	FNET	An-TR,TL-TR	–	An-TR,Ce-TR,TL-TR	0.28: An-TR
		Cluster – whole AD group		Cluster – probable AD group	
Static canonical correlation		Cluster $p < 0.0036$	Highest R^2	Cluster $p < 0.0036$	Highest R^2
Mean coeff.	RSEC	None	–	Ce-TL	–
	FNET	An-Po, Ce-TL, AT-PT	–	All except An-Ce,An-TR,Ce-Po,TL-TR	0.41: Ce-TL

Complexity		2nd component – whole AD group		2nd component – probable AD group	
		Cluster $p < 0.0036$	Highest R^2	Cluster $p < 0.0036$	Highest R^2
Auto-m inform.	RSEC	All except An	0.31: L	All except An	0.42: L
	FNET	Po-Te,Te/R	0.21: Po-Te	Po-Te,L	0.27: Po-Te
		Sites $p < 0.0036$	Highest R^2	Sites $p < 0.0036$	Highest R^2
Shan. entropy	RSEC	T7, T8	0.27: T7	F7, T7, T8	0.39: T7
	FNET	T7, P4	–	None	–
Tsallis entropy	RSEC	T7, T8	0.24: T7	F7, T7,T8	0.36: T7
	FNET	T7,P8	–	T7	–

RSEC: resting state with eyes closed; FNET: face–name encoding task.
Highest R^2: only values >0.2 reported.
Electrode sites: Fp1, Fp2, F3, F4, Fz, T7, T8, F7, F8,C3, C4, Cz, P3, P4, P7, P8, Pz, O1, O2; FCz: between Fz and Cz.
Electrode clusters: anterior (An): Fp1, Fp2, F3, F4; central (Ce): Fz, Cz, Pz, C3, C4; temporal (Te): F7, T7, P7 (left side) and F8, T8, P8 (right side); posterior (Po): P3, P4, O1, O2; posterior-temporal (Po-Te): P7, P3, O1, P8, P4, O2, anterior-temporal (An-Te): Fp1, F3, F7, Fp2, F4, F8.

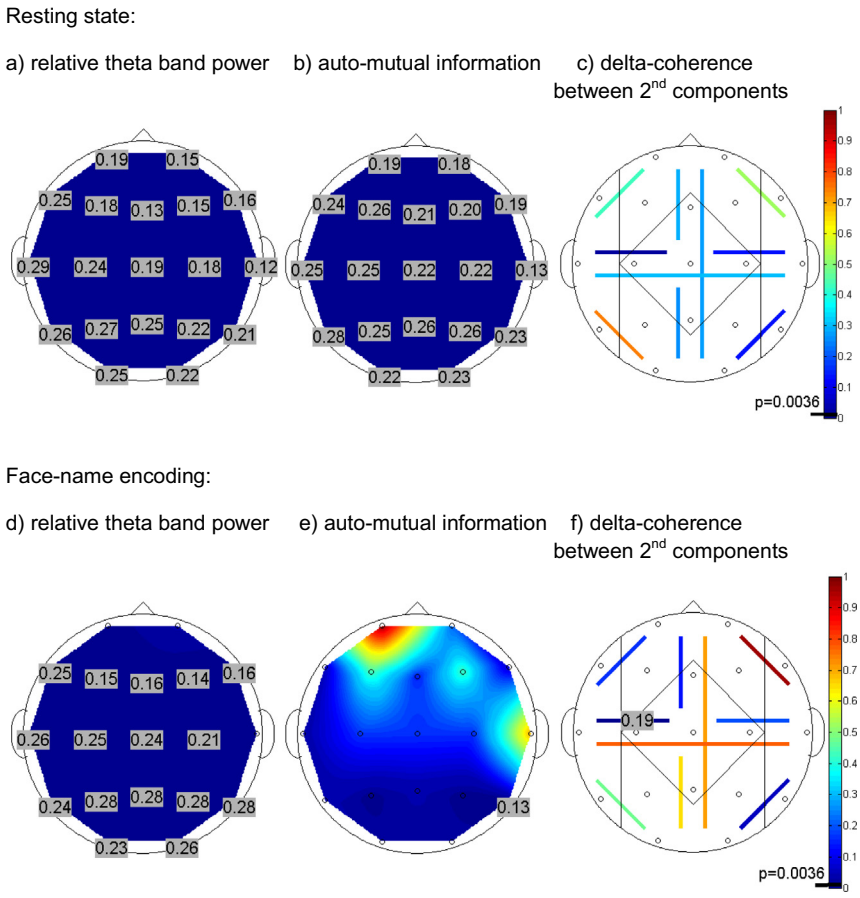

Fig. 1. Electrodes and electrode clusters with statistically significant results ($p < 0.0036 = 0.05/14$) and coefficients of determination for electrode sites and 1st/2nd components of electrode clusters. Color: Significance; blue: significant ($p < 0.0036$), red: not significant. Numbers: maximum coefficients of determination (given in case of significant result only).

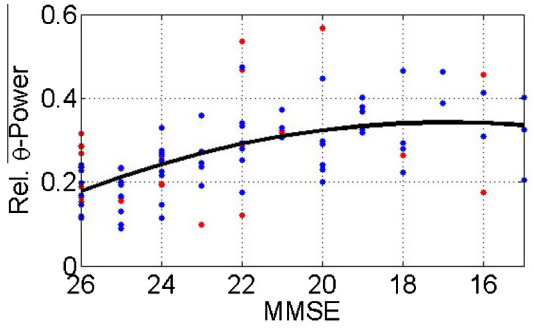

Fig. 2. Relative theta band power for the left-side electrode cluster (second component). Face–name encoding task: blue: probable AD; red: possible AD Regression: all AD: $p = 5.10^{-6}$, $R^2 = 0.33$ (black line); probable AD: $p = 6.10^{-10}$, $R^2 = 0.51$.

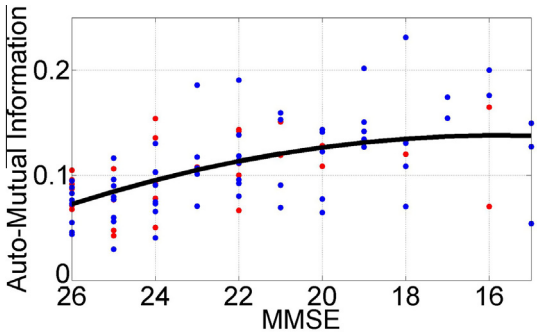

Fig. 3. Auto-mutual information for the left-side electrode cluster (second component). Resting state with eyes closed: blue: probable AD; red: possible AD Regression: all AD: $p = 4.46.10^{-8}$, $R^2 = 0.31$ (black line); probable AD: $p = 5.09.10^{-8}$, $R^2 = 0.42$.

MMSE scores also explained 31% of the variation in auto-mutual information (RSEC) in the second principal component of the left-side electrode cluster. Auto-mutual information also increased with decreasing MMSE score as shown in Fig. 3.

Furthermore, MMSE scores explained 27% of Shannon entropy (RSEC, increasing), and 25% of alpha (8–13 Hz, RSEC, decreasing) and beta1 (13–20 Hz, FNET, decreasing) relative band powers. Coefficients of determination reached 24% for Tsallis entropy (RSEC, decreasing), and 21% for delta relative band power (2–4 Hz, RSEC, increasing).

For synchrony measures, coefficients of determination reached less than 20%. Both coherence and canonical correlation increased with decreasing MMSE score in the range of 20 to 26, but decreased in the range of 15–20. Fig. 4 shows the scatter plot with regressions for coherence.

MMSE scores explained 25% of the variations in the overall QEEG factor. This result is shown in Fig. 5.

3.2. Probable AD

Significantly higher coefficients of determination were found for those patients with probable AD. Again, the highest coefficient of determination was found for theta relative band power, where 51% of the variations in this marker were explained by MMSE scores.

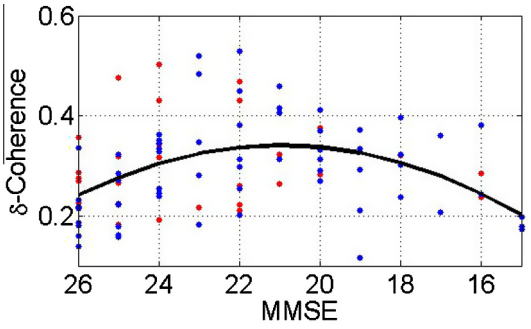

Fig. 4. Coherence (delta), 2nd component, central-left temporal electrode cluster. Face–name encoding task: blue: probable AD; red: possible AD Regression: all AD: $p < 0.0016$, $R^2 = 0.19$ (black line); probable AD: $p = 8.10^{-7}$, $R^2 = 0.38$.

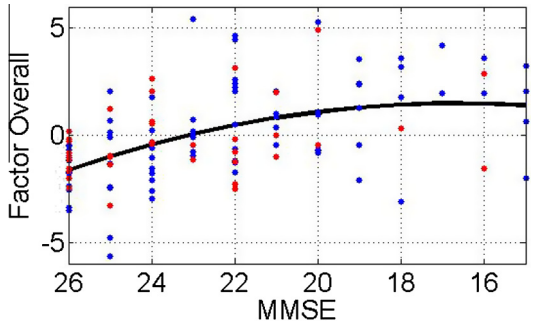

Fig. 5. Overall QEEG factor. Blue: probable AD; red: possible AD Regression: all AD: $p = 0.0002$, $R^2 = 0.25$ (black line); probable AD: $p = 2.10^{-5}$, $R^2 = 0.31$.

Auto-mutual information was again the second-best QEEG marker with a coefficient of determination of 42%. Granger causality, canonical correlations and delta coherence reached 41%, followed by Shannon entropy with a coefficient of determination of 39%. Tsallis entropy reached 36% and alpha relative band power 24%. For the overall QEEG factor, MMSE scores explained 31% of its variation.

3.3. Discriminative power of regressions

For diagnostic purposes, strong changes in QEEG markers with decreasing MMSE scores would be desired. Table 3 lists relative slopes of regression at MMSE scores of 26, 20 and 15. Relative slopes were calculated as the absolute value of the slope of the tangent of the quadratic regression line at MMSE scores of 26, 20 and 15 divided by the corresponding ordinate value. The steepest slopes were found for relative theta band power, coherence and auto-mutual information at an MMSE score of 26. At lower MMSE scores, slopes were much less steep with the exception of coherence at MMSE scores around 15. Unfortunately, however, the values for coherence and correlation markers were ambiguous, as shown in Fig. 4.

Specifically for the whole AD group the slope (at MMSE = 26) for the overall QEEG factor was 39.3%, for relative theta band power 18.8%, for delta coherence 14.8%, and for auto-mutual information 16.6%.

For probable AD the slope for overall QEEG factor was 34.5%, for relative theta band power 24.6%, for delta coherence 23.3%, and for auto-mutual information 21.6%.

3.4. Summary of most significant results

Table 4 gives a rating of the QEEG markers found in this study with respect to relative slope of the regressions and coefficients of determination and shows that face–name encoding was superior to resting state for relative theta and beta band power, for coherence and canonical correlation.

4. Discussion and conclusions

This so far largest study of QEEG markers for frequency slowing, altered synchrony and reduced complexity versus disease severity in AD shows theta relative band power measured during face encoding to be most closely related to AD severity. MMSE scores explained 38% of the variation in theta relative band power for the entire group of probable and possible AD cases and 50% in those with probable AD. Theta relative band power determined during face encoding yielded the highest coefficients of determination. All other QEEG measures including other relative band powers, synchrony and complexity measures were less closely related to disease severity, but it was always the left-sided indices in temporal and parietal regions that consistently showed most significant results in our patients. It is noteworthy that the overall QEEG factor resulted in lower coefficients of determination of disease severity than did individual QEEG measures including relative alpha and beta1 band powers and complexity measures. Also in the probable AD group, synchrony measures yielded higher coefficients of determination than did the respective overall QEEG factor.

Nonetheless, the overall QEEG factor exhibited steeper regression slopes. This means that it discriminates better between patients with various disease severities than do frequency slowing, synchrony or complexity.

Although numerous studies have compared QEEG markers of AD patients and those of normal controls, very little information is available on associations between QEEG markers and disease severity in AD. In line with our data van der Hiele et al. (2007) reported results for relative theta power during eyes closed versus Cambridge Cognitive Examination (CAMCOG) total score and CAMCOG language test (Roth et al., 1986) in 16 patients with probable AD and 22 controls. The authors found theta relative power to be increased in AD patients as compared to controls and to relate to decreased performance in all cognitive domains. Coefficients of determination were $R^2 = 0.18$ for relative theta power versus CAMCOG total score and $R^2 = 0.24$ for relative theta power versus CAMCOG language test.

Babiloni et al. (2006) compared Loreta current densities of 126 normal elderly subjects, 155 patients with mild cognitive impairment and 193 patients with mild AD in resting state with eyes closed. MMSE scores ranged between 17 and 30. Regressions for Loreta current densities versus MMSE yielded a coefficient of determination (R^2) of 0.03 for occipital delta. For alpha 1, R^2 was calculated as 0.02 (parietal), 0.04 (occipital), 0.02 (temporal) and 0.03 (limbic).

Lee et al. (2010) showed results for global synchronization index (GSI) as a biological correlate of cognitive decline. The GSI values in the beta1, beta2, beta3, and gamma bands were significantly lower in AD patients than in controls and correlated positively with MMSE scores in all participants. In AD patients, GSI values were negatively correlated with MMSE scores in the delta bands, but positively correlated in the beta1 and gamma band. For the AD patients, Spearman's rho was 0.46 for low beta GSI values versus MMSE and 0.51 for gamma GSI values versus MMSE.

Kwak (2006) investigated quantitative EEG in different stages of Alzheimer's disease in 146 AD patients (10 CDR = 0.5, 37 CDR = 1, 47 CDR = 2, 52 CDR = 3) and 34 controls. Consistent correlations between relative band powers and CDR were found, i.e. an increase in delta and theta and a decrease in alpha and beta intensities. No

Table 3
Relative slope of the regressions.

Relative slope	Probable AD			All AD		
QEEG marker	26	20	15	26	20	15
Theta relative band power	24.64%	3.17%	−1.55%	18.80%	3.17%	−1.54%
Alpha relative band power	−5.53%	−6.36%	−7.00%	−6.99%	−5.10%	−1.82%
Beta1 relative band power	−7.42%	−4.57%	−0.23%	−7.15%	−4.63%	−0.73%
Delta coherence	23.28%	−3.42%	−21.80%	14.84%	−3.40%	−17.50%
Conditional Granger causality	−9.19%	−3.28%	4.40%	−8.82%	−1.35%	6.17%
Static canonical correlation	5.49%	−0.62%	−4.51%	3.31%	−0.84%	−3.68%
Auto mutual information	21.59%	4.27%	−0.21%	16.63%	3.71%	−0.14%
Shannon entropy	0.44%	0.25%	0.14%	0.37%	0.20%	0.09%
Tsallis entropy	0.68%	0.37%	0.17%	0.50%	0.29%	0.14%
Overall QEEG factor	34.51%	24.47%	−1.48%	39.27%	18.43%	−5.20%

Table 4
Rating of QEEG markers with respect to relative slope of regressions and coefficients of determination.

QEEG Marker	Rating	Best Paradigm	All AD relative slope at MMSE = 26	R^2	Probable AD relative slope at MMSE = 26	R^2
Relative theta band power	+	Face–name	18.8%	0.33	24.6%	0.51
Relative alpha band power	–	Resting state	−7.0%	0.21	−5.5%	0.24
Relative beta1 band power	–	Face–name	−7.2%	0.25	−7.4%	0.35
Coherence *AMBIGUOUS*	–	Face–name	14.8%	<0.20	23.3%	0.41
Can correlation *AMBIGUOUS*	–	Face–name	3.3%	<0.20	5.5%	0.41
Granger causality	–	Resting state	−8.8%	<0.20	−9.2%	0.41
Auto-mutual information	+	Resting state	16.6%	0.31	21.6%	0.42
Shannon entropy	–	Resting state	0.4%	0.27	0.4%	0.39
Tsallis entropy	–	Resting state	0.5%	0.24	0.7%	0.36
Overall QEEG factor	+	Combination	39.5%	0.25	34.5%	0.31

coefficients of determination or other measures of dependence were given.

Our findings are in accordance with those of van der Hiele et al. (increased relative theta band power associated with decreased cognitive performance) and Kwak (consistent correlations between relative band powers and CDR). In contrast to van der Hiele et al., our study shows significantly higher coefficients of determination, namely up to 50% as compared to 24% in their investigation.

Our study has several strengths. With 118 AD patients our investigation is the largest QEEG study of mild to moderate AD without using normal controls. We developed optimized signal preprocessing methods to extract true brain signals and remove artifacts from eye movement and blinking and from heartbeat-induced interference. Moreover, we applied an indirect spectral estimator to determine multivariate signal spectra of short epochs that provided lower variances for large samples than does the commonly used periodogram. All analyses were adjusted for possible confounding by age, sex, duration of dementia, and level of education.

This is the first AD study to use both resting state with eyes closed and a face–name encoding task as cognitive state for the assessment of QEEG markers; it determined not only spectral band powers, but also synchrony and complexity measures.

In summary, our data indicate that specific QEEG markers of slowing, synchrony and complexity relate closely to AD severity in patients with MMSE scores between 15 and 26. The steepest regression slope is found in the MMSE score range between 20 and 26. Our data also demonstrate that, for certain QEEG markers, EEG assessments during cognitive states are more informative than are those obtained during resting state. Theta relative band power measured during face encoding was most closely related to the cognitive performance of study participants. Considering both slope (ability of the marker to distinguish between different disease severities) and coefficient of determination from quadratic regression, the best ranking was found for relative theta power, auto-mutual information and overall qEEG factor.

We fully realize that longitudinal studies are now warranted to determine whether theta relative band power during face encoding can also aid in predicting AD progression. Moreover, it will also be important to determine the role of QEEG markers as putative predictors of disease progression as compared to other potential markers including CSF and functional as well as structural imaging markers.

Acknowledgment

This project was sponsored by a grant from the Austrian Research Promotion Agency FFG, project no. 827462, including financial contributions from Dr. Grossegger and Drbal GmbH, Vienna, Austria.

Conflict of interest: None of the authors have potential conflicts of interest to be disclosed.

References

Babiloni C, Binetti G, Cassetta E, Dal Forno G, Del Percio D, Ferreri F, et al. Sources of cortical rhythms change as a function of cognitive impairment in pathological aging: a multicenter study. Clin Neurophysiol 2006;117:252–68.
Brillinger DR. Time Series: Data Analysis and Theory. Holden-Day; 1981.
Chandler MJ, Lacritz LH, Hynan LS, Barnard HD, Allen G, Deschner M, Weiner MF, et al. A total score for the CERAD neuropsychological battery. Neurology 2005;65(1). 102-6.
Coben LA, Danzinger W, Storandt M. A longitudinal EEG study of mild senile dementia of Alzheimer type: changes at 1 year and at 2.5 years. Electroencephalogr Clin Neurophysiol 1985;61:101–12.
Cover TM, Thomas JA. Elements of Information Theory. New York: Wiley; 1991.
Dauwels J, Vialette F, Musha T, Cichocki A. A comparative study of synchrony measures for the early diagnosis of Alzheimer's disease based on EEG. Neuroimage 2010;49:668–93.
Drago V, Babiloni C, Bartrés-Faz D, Caroli A, Bosch B, Hensch T, et al. Disease tracking markers for Alzheimer's disease at the prodromal (MCI) stage. J Alzheimer's Dis 2011;26:159–1999.
Draper NR, Smith H. Applied Regression Analysis. Wiley Series in Probability and Statistics; 1966.
Flamm C, Kalliauer U, Deistler M, Waser M, Graef A. Graphs for dependence and causality in multivariate time series. In: Wang L, Garnier H, editors. System Identification, Environmental Modelling, and Control System Design. London: Springer; 2012. p. 133–51.

Folstein MF, Folstein SE, McHugh PR. Mini–Mental State. A practical method for grading the cognitive state of patients for the clinician. J Psychiatr Res 1975;12:189–98.
Giannakopoulos P, Missonnier P, Gold G, Michon A. Electrophysiological markers of rapid cognitive decline in mild cognitive impairment. Dementia in Clinical Practice. Front Neurol Neurosci 2009;24:39–46.
Granger CWJ. Investigating causal relations by econometric models and cross-spectral methods. Econometrica 1969;37:424–38.
Hidasi Z, Czigler B, Salacz P, Csibri E, Molnar M. Changes of EEG spectra and coherence following performance in a cognitive task in Alzheimer's disease. Int J Psychophysiol 2007;65:252–60.
Hogan MJ, Swanwick GRJ, Kaiser J, Rowan M, Lawlor B. Memory-related EEG power and coherence reductions in mild Alzheimer's disease. Int J Psychophysiol 2003;49:147–63.
Hotelling H. Analysis of a complex of statistical variables into principal components. J Educ Psychol 1933;24(417–441):498–520.
Hotelling H. Relations between two sets of variates. Biometrika 1936;28:321–77.
Jeong J. EEG dynamics in patients with Alzheimer's disease. Clin Neurophysiol 2004;115:1490–505.
Kwak YT. Quantitative EEG findings in different stages of Alzheimer's disease. J Clin Neurophysiol 2006;23:456–61.
Lawley DN. The estimation of factor loadings by the method of maximum likelihood. Proc R Soc Edinb 1940;60:64–82.
Lee S-H, Park Y-M, Kim D-W, Im C-H. Global synchronization index as a biological correlate of cognitive decline in Alzheimer's disease. Neurosci Res 2010;66:333–9.
Leiser SC, Dunlop J, Bowlby MR, Devilbiss DM. Aligning strategies for using EEG as a surrogate biomarker: a review of preclinical and clinical research. Biochem Pharmacol 2011;81:1408–21.
McKhann G, Drachmann D, Folstein M, Katzman R, Price D, Stadlan EM. Clinical diagnosis of Alzheimer's disease: report of the NINCDS-ADRDA Work Group under the auspices of Department of Health and Human Services Task Force on Alzheimer's Disease. Neurology 1984;34:939–44.
Menendez M. Down syndrome. Alzheimer's disease and seizures. Brain Dev 2005;27:246–52.
Pijnenburg YAL, Made Yvd, van Cappellen von Walsum AM, Knol DL, Scheltens Ph, Stam CJ. EEG synchronization likelihood in mild cognitive impairment and Alzheimer's disease during a working memory task. Clin Neurophysiol 2004;115:1332–9.
Platt B, Riedel G. The cholinergic system. EEG and sleep, Behav Brain Res 2011;221:499–504.
Rosen WG, Mohs RC, Davis KL. A new rating scale for Alzheimer's disease. Am J Psychiatry 1984;141:1356–64.
Rosenberg JR, Amjad AM, Breeze P, Brillinger DR, Halliday DM. The Fourier approach to the identification of functional coupling between neuronal spike trains. Prog Biophys Mol Biol 1989;53:1–31.
Rossini PM, Rossi S, Babiloni C, Polich J. Clinical neurophysiology of aging brain: from normal aging to neurodegeneration. Prog Neurobiol 2007;83:375–400.
Roth M, Tym E, Mountjoy CQ, Huppert FA, Hendrie H, Verma S, et al. CAMDEX. A standardised instrument for the diagnosis of mental disorder in the elderly with special reference to the early detection of dementia. Br J Psychiatry 1986;149:698–709.
Sakkalis V. Review of advanced techniques for the estimation of brain connectivity measured with EEG/MEG. Comput Biol Med 2011;41:1110–7.
Santos SF, Pierrot N, Octave JN. Network excitability dysfunction in Alzheimer's disease: insights from in vitro and in vivo models. Rev Neurosci 2010;21:153–71.
Seiler S, Schmidt H, Lechner A, Benke T, Sanin G, Ransmayr G, et al. Driving cessation and dementia: results of the Prospective Registry on Dementia in Austria (PRODEM). PLoS ONE 2012;7:e52710.
Shannon CE. A mathematical theory of communication. Bell Syst Tech J 1948;27:379–423.
Soininen H, Partanen J, PääkkÖnen A, Koivisto E, Riekkinen PJ. Changes in absolute power values of EEG spectra in the follow-up of Alzheimer's disease. Acta Neurol Scand 1991;83:133–6.
Tsallis C. Possible generalization of Boltzmann-Gibbs statistics. J Stat Phys 1988;52:479–87.
Uhlhaas PJ, Singer W. Neural synchrony in brain disorders: relevance for cognitive dysfunction and pathophysiology. Neuron 2006;52:155–68.
van der Hiele K, Vein AA, Reijntjes RHAM, Westendorp RGJ, Bollen ELEM, van Buchem MA, et al. EEG correlates in the spectrum of cognitive decline. Clin Neurophysiol 2007;118:1931–9.
Waser M, Garn H. Removing cardiac interference from the electroencephalogram using a modified Pan-Tompkins algorithm and linear regression. 35th IEEE Int'l. Conf. Engineering in Medicine & Biology, Osaka, 3–7 July 2013, Proceedings. p. 2028–2031.
Waser M, Deistler M, Garn H, Benke T, Dal-Bianco P, Ransmayr G, et al. EEG in the diagnostics of Alzheimer's disease. Stat Pap 2013;54:1095–107.